Proceedings of the 7th International Symposium on Marine Engineering
Tokyo, October 24th to 28th, 2005

# Development of Turtle-like Submergence Vehicle

**Akihisa KONNO*, Takuro FURUYA**, Akisato MIZUNO***, Kazuhisa HISHINUMA***,
Koichi HIRATA**** and Masakuni KAWADA******

**ABSTRACT**

A submergence vehicle based on sea turtles was developed. This vehicle has two fore fins with two degrees of freedom; flapping and feathering motions, and flaps for propulsion and/or maneuvering. Hind fins were also equipped, and a buoyancy controller for the vehicle was designed. In experiments this vehicle swam at 0.06 m/s when fore fin frequency was 0.53 Hz.

Performance of the vehicle was also estimated using the blade element theory. By applying the theory against our vehicle, its velocity is estimated as around 0.18 m/s when fin frequency is 0.53 Hz. Two of the reasons of difference between the theory and the experiment are that the theory ignores wing-tip loss so that it gives the higher estimation than expected, and that the vehicle could not perform its full potential at the experiment. This vehicle still has many problems, and by taking measure of them the vehicle may be used to estimate the possibility of this kind of vehicles.

**Key Words**: Sea Turtle, Submergence Vehicle, Feathering Motion, Blade Element Theory

## NOMENCLATURE

| | |
|---|---|
| $C(r)$: | Chord length at span position *r* [m] |
| $C_L(\alpha)$: | Lift coefficient of blade elements with given angle of attack |
| $C_D(\alpha)$: | Drag coefficient of blade elements with given angle of attack |
| $L$: | Body length of an aquatic animal or a vehicle [m] |
| $r$: | Span position [m] |
| $R_0$: | Root position of fin from rotational center [m] |
| $R_t$: | Tip position of fin from rotational center [m] |
| $T$: | Feathering period[s] |
| $Th$: | Thrust [N] |
| $Tq$: | Torque to swing a fin [N.m] |
| $U$: | Vehicle velocity (uniform flow velocity) [m/s] |
| $V(r,t)$: | Flow velocity relative to a wing element [m/s] |
| $\alpha(r,t)$: | Relative angle of attack [rad] |
| $\beta(t)$: | Feathering angle [rad] |
| $\beta_{max}$: | Maximum feathering angle [rad] |
| $\gamma(r,t)$: | Inflow angle [rad] |
| $\phi$: | Phase delay from flapping angle to feathering angle [rad] |
| $\rho$: | Density of fluid [kg/m$^3$] |
| $\theta(t)$: | Flapping angle [rad] |
| $\theta_{max}$: | Maximum flapping angle [rad] |
| $\omega(t)$: | Flapping angular velocity [rad/s] |

* Kogakuin University,
Nakano-machi 2665, Hachioji-shi, Tokyo 192-0015, JAPAN
FAX: +81-426-28-4156, E-mail: konno@researchers.jp
** Fuji Yusoki Kogyo Co., Ltd.
*** Kogakuin University
**** National Maritime Research Institute

## 1. INTRODUCTION

Fish swimming has become one of interesting research topics in the field of marine engineering. Both fundamental analysis of the mechanism of fish swimming and application to propulsion and/or maneuvering have been studied by many researchers [1]. We have also studied this topic, and developed several fish-like underwater vehicles [2][3]. There may be potentially many demands of underwater vehicles so that further studies of fish swimming may well be done.

For applying to underwater vehicles, a swimming style in which many parts of the body are used, like that of eels and many freshwater fish, is not appropriate very much, because it is hard to realize that motion with mechanics. On this standpoint, we directed our attention to feathering motion of fins which is used by, for example, rays, turtles and penguins. These creatures do not, at least widely, deform the body and mainly use a pair of fins for propulsion and maneuvering. This feature fits for the development of underwater robots.

Recently we studied the feathering motion of sea turtles, and developed a turtle-like submergence vehicle. In this paper we report the feature and performance of the vehicle.

## 2. DEVELOPMENT OF SUBMERGENCE VEHICLE BASED ON SEA TURTLE

### 2.1 Sea Turtle

Fig. 1 shows a photograph of a sea turtle (loggerhead turtle). Sea turtles live in the ocean in nearly all their lifetime, except

**Fig. 1: Sea Turtle (Loggerhead Turtle)**

when they are born or they spawn eggs. For this reason, sea turtles have features that fit for the underwater life. A sea turtle has two pairs of fins. One is fore fins, which are large and elastic, and has two joints which correspond to shoulder and elbow. The other is hind fins which are small. It mainly uses the fore fins for propulsion and maneuvering, and uses the hind fins as a rudder or for support of maneuvering. The body is covered by a hard shell, and it deforms little or nothing. This feature is good for applying to underwater vehicles. A sea turtle has a bladder.

### 2.2 Modeling of Flapping and Feathering Motion

Fore fins are both the main thruster and rudder of sea turtles. To model these swimming for our submergence vehicle, it is important to realize the essence of their fore fin motion.

In our underwater robots, the fin motion of sea turtles is simplified. A sea turtle has two joints on each fore fin, while our vehicle has only one. This joint has two degree of freedom: swing and twisting motion. Swing motion realizes flapping (beating) of the fin. Twisting motion realizes so-called "feathering motion", which dynamically changes angle of attack of the fin. As a result of observing swimming of a few sea turtles in an aquarium, we thought that these two motions were essence of movement of fore fins of sea turtles.

Structure of the joint will be explained later.

### 2.3 General Structure of Turtle-like Submergence Vehicle

Fig. 2 shows a photograph of a turtle-like submergence vehicle we developed, named "Turtle 2005". Fig. 3 shows its general structure. Structure of fore fins will be explained in the next subsection and is not explained here. Each hind fin is directly connected to an R/C servomotor. All of the motors can be independently controlled each other.

The backbone part of the vehicle is made of three boxes, hereafter called Box 1, 2 and 3, which are made of acrylic resin and are watertight using silicon gasket packing. In Box 1 a battery is installed. Mechanisms of motion of fore fins, control circuits and a bladder system are installed in Box 2. In Box 3 the R/C servomotors for hind fins, another battery and an R/C receiver is installed. The placement and control of gravity center, and the body shape are considered to design and arrange these boxes. These boxes are connected each other with silicon tubes through which electric cables are laced, and are covered by an outer cover made of FRP. The outer cover is shaped as teardrop form to suppress fluid drag.

### 2.4 Mechanism and Motion of Fore Fins

Fig. 4 shows the structure of the joint part of the fore fins. As is explained in Section 2.2, we decided to make each fore fin to have two degree of freedom; swinging (flapping) and twisting (feathering) motions.

For swinging motion, we made use of a stepping motor, a

**Fig. 2: Submergence Vehicle "Turtle 2005"**

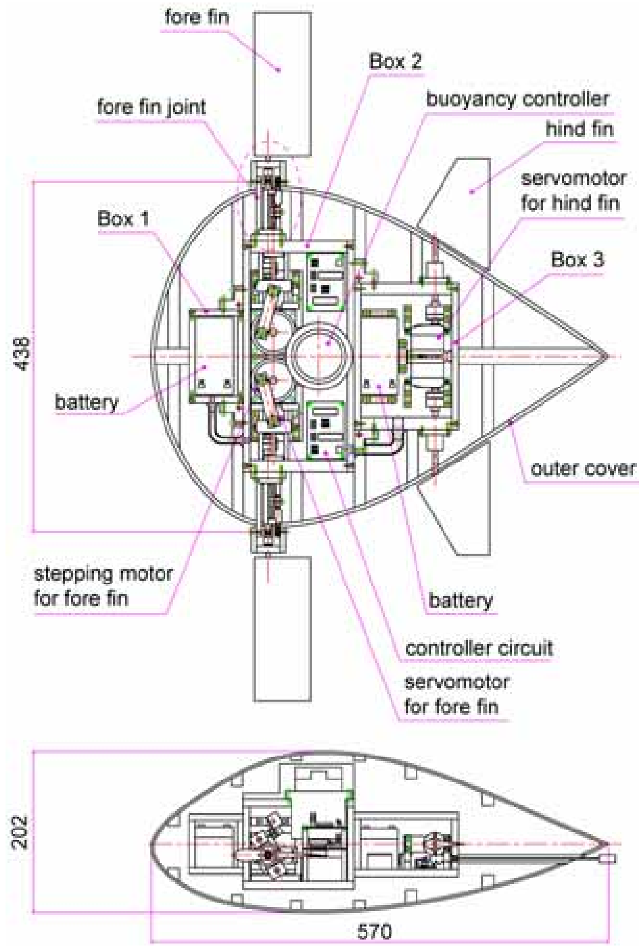


**Fig. 3: Structure of Turtle-like Submergence Vehicle**

crank mechanism and a universal joint for each fin. These fore fins are designed to swing around $\pm 45$ deg. To make this motion possible, a linear shaft is connected on each crank and the shaft is installed with a solid linear bearing on the shelf of Box 2 for waterproof. As the stroke of linear shafts is large, it is not appropriate to adopt rubber bellows that is often used for R/C boats.

To suppress friction force inside these linear bearings, it is necessary to reduce sideway movement of the shaft. For this purpose, guide shafts are installed both inside and outside of Box 2.

For twisting motion, an R/C servomotor is directly connected to the shaft for each fin. Fins can be exchanged.

### 2.5 Control of Turtle-like Submergence Vehicle

To produce thrust force by flapping fore fins, flapping and feathering motion must be operated in cooperation each other.

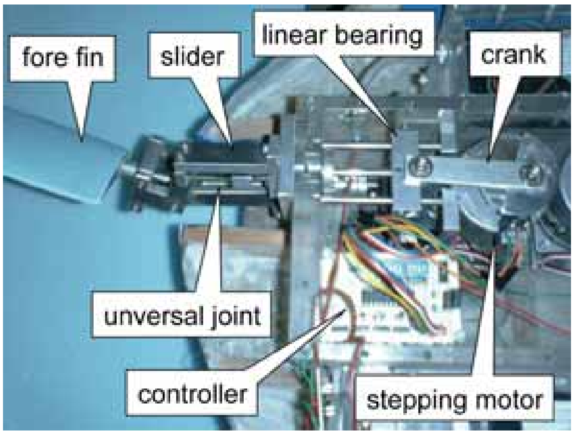


(a) Appearance

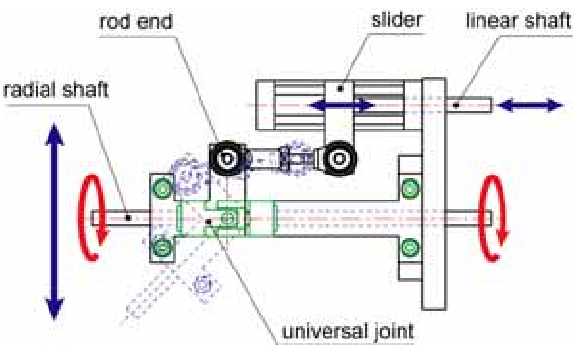


(b) Illustration of structure

**Fig. 4: Structure of Fore Fin Joint**

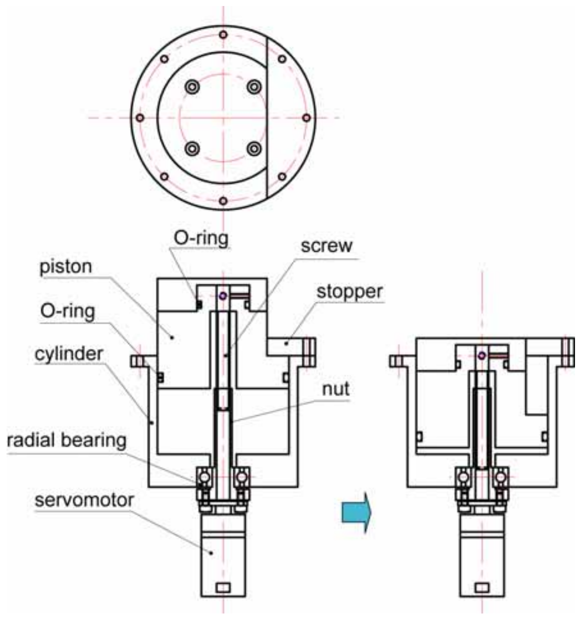


**Fig. 5: Structure of Buoyancy Controller**

In our vehicle, two controllers are installed; one is for flapping motion and the other for feathering. A one-chip microprocessor (Atmel AVR AT90S2313-10PC) is installed on each controller. These can be operated either independently or in cooperation.

On the shaft of stepping motor of a fore fin, two pairs of a cam disk and a micro switch are installed. By monitoring conditions of these switches, angle of flapping is roughly obtained. The controller for feathering angle monitors these switches, and controls the angle of the corresponding servomotor.

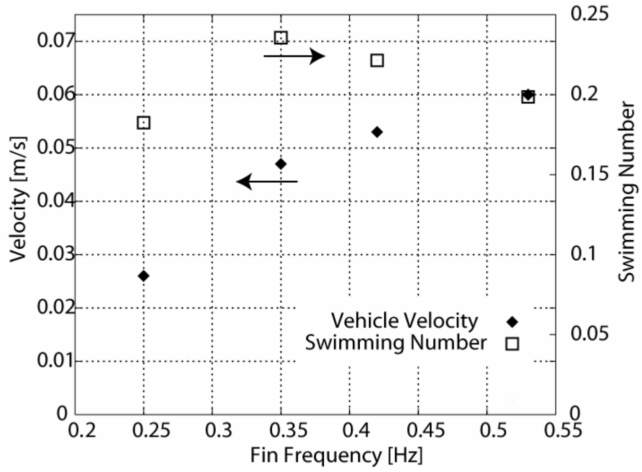


**Fig. 6: Swimming Velocities and Swimming Numbers as Functions of Flapping Frequencies**

The hind fins are also controlled by controllers with microprocessors, one for each fin. These are intended to support maneuvering operation.

### 2.6 Buoyancy Controller

To control buoyancy of the vehicle to assist diving and surfacing operation, this vehicle is designed that it can embed a buoyancy controller. Fig. 5 shows the planned structure of a buoyancy controller to be embedded to the vehicle. This has a pair of a piston and a cylinder. The piston can be inserted into or extracted from the cylinder by rotating a screw by a servomotor, so that the volume changes and hence the buoyancy changes. The vehicle has a room for this mechanism, but the controller is not implemented yet.

## 3. EXPERIMENTS

Experiments are held at Fish Robot Experiment Basin at National Maritime Research Institute. In the experiments the submergence vehicle swam near water surface, varying frequencies of feathering motion of fore fins. In these experiments simple two-dimensional hydrofoils were adopted for fore fins. Cross sections of the fore fins were NACA0015 hydrofoil and were uniform to span direction. Span and chord length of each fin are 180 mm and 70 mm, respectively.

Fig. 6 shows swimming velocities of the vehicle against the flapping frequencies. It is shown that the velocity was increased when the frequency was increased, and at the highest frequency of 0.53 Hz the maximum velocity, 0.06 m/s, was obtained.

Fig. 6 also shows the swimming number, *Sw*. The swimming number was a non-dimensional parameter to estimate swimming performances of aquatic animals, and is defined as

$$Sw = \frac{U}{Lf}, \qquad (1)$$

where $U$ is swimming velocity, $L$ is body length and $f$ is the frequency of a fin. This number is often used to evaluate the performance of fish that swim with tail fins. The swimming number of the turtle-like vehicle was around 0.24 at the maximum when the frequency of fins is 0.35 Hz. This is roughly same as those of fish-like robots made by our group.

This vehicle cannot dive into underwater because of the absence of a buoyancy controller (and its weight), so that it could only swim near water surface. For this reason, the fore fins periodically came out on water and did not always paddle water; that decreased the performance. In addition, the motion of fins was not optimized. Therefore there is still room of improvements on this vehicle.

## 4. FUNDAMENTAL ANALYSIS OF PERFORMANCE OF FLAPPING FINS

### 4.1 Blade Element Theory for Flapping Fins

To estimate the performance of the turtle-like submergence vehicle, blade element theory was adopted to the feathering motion of fore fins. Here we adopt rather simple version of this theory; more complicated treatment that considers deformation of fins will be shown by Hishinuma et al. [4].

In blade element theory, a fin is divided into wing blade elements with infinitesimal span width, and fluid force affecting on each elements is considered. In our analysis the following things are assumed.

1. Performance of a wing element, which is represented as a combination of lift and drag coefficients, is same as that in stable condition. Dynamic effect is not considered.
2. Wing-tip loss can be ignored.
3. Fins are rigid, and are flapped periodically in a certain plane normal to the swimming direction.

Under these assumptions, and under definitions of variables as shown in Fig. 7, the thrust and torque produced by a flapping wing is expressed by the following equations, respectively.

$$Th = \int_{R_0}^{R_t} \left(C_L \sin\gamma - C_D \cos\gamma\right) \frac{1}{2} \rho V^2 C(r)\, dr \qquad (2)$$

$$Tq = \int_{R_0}^{R_t} \left(C_L \cos\gamma + C_D \sin\gamma\right) \frac{1}{2} \rho V^2 C(r) r\, dr \qquad (3)$$

Here $C_L$ and $C_D$ are not constant, but functions of angle of attack $\alpha$. $\omega(t)$ is an angular velocity of flapping motion which expression will be given later.

$V$ is the flow velocity relative to the wing element, and is calculated as follows:

$$V(r,t) = \sqrt{U^2 + \left(r\omega(t)\right)^2} \qquad (4)$$

Inflow angle $\gamma$ is calculated as follows:

$$\gamma(r,t) = \tan^{-1} \frac{r\omega(t)}{U} \qquad (5)$$

As flapping motion is periodic, flapping angle, $\theta(t)$, and angular velocity, $\omega(t)$, are given by the following equations, respectively.

$$\theta(t) = \theta_{\max} \sin \frac{2\pi}{T} t \qquad (6)$$

$$\omega(t) = \frac{d\theta(t)}{dt} = \frac{2\pi}{T} \theta_{\max} \cos \frac{2\pi}{T} t \qquad (7)$$

Feathering angle $\beta$ is given as follows:

$$\beta(t) = \beta_{\max} \sin\left(\frac{2\pi}{T} t - \phi\right) \qquad (8)$$

Here $\phi$ represents phase delay of the feathering angle against the flapping motion, and is assumed constant.

The angle of attack $\alpha$ is given as $\alpha(r,t) = \gamma(r,t) - \beta(t)$.

### 4.2 Estimation of Fluid Force and Comparison with Experimental Results

Using the above theory, velocity of the vehicle is estimated under the condition same as that in the experiments in Section 3. In the following calculation, we made use of lift and drag coefficients of NACA0015 airfoil under condition that Reynolds number is 80000; that data were given by Sheldahl and Klimas [5]. Reynolds number of the experiments is around 4000, but appropriate data for this condition is not obtained so that the above data were used. Maximum flapping angle is $\pi/4$ and is constant.

The thrust calculated by Eq. (2) should balance with drag force affecting on the vehicle. The drag is calculated using the following equation.

$$D = C_D \cdot A \cdot \frac{1}{2} \rho U^2 \qquad (9)$$

Here $C_D$ is the drag coefficient of the vehicle and $A$ is the projection area of the body: $A$=0.06 m$^2$. As it is difficult to accurately estimate the drag force, we roughly assumed that the body drag is dominant, and that its drag coefficient is equal to that of a teardrop: $C_D$=0.05.

Fig. 8 shows calculated thrust and drag forces under conditions that the flapping frequency is 0.53 Hz. Thrust forces are calculated varying the feathering angle. A certain point where a thrust line (colored) and the drag line (black) cross corresponds to estimated velocity the vehicle will swim under given condition. In the experiment, the feathering angle was $\pi/4$ and at that condition the vehicle velocity is estimated around 0.18 m/s.

This is around three times as fast as the experimental result, 0.06 m/s. This may be because of the following reasons.

1. As the wing-tip loss is not considered, the numerical estimation gives higher thrust than that in the real situation.
2. As is mentioned in Section 3, the experimental condition was not ideal; especially the fins did not always paddle water.
3. Drag coefficient of the body is not appropriate.

For the above-mentioned reasons this estimation cannot be trusted yet, and improvements are required.

Estimation of flapping torque is not yet done, and is the future subject.

## 5. CONCLUSIONS

A submergence vehicle which models a sea turtle is developed. Its performance is estimated by blade element theory. To estimate the performance of the turtle-like submergence vehicle, blade element theory was adopted. With numerical and experimental analysis, the following conclusions are obtained.

1. The mechanism of fore fins can perform essential motion of that of a real sea turtle.
2. Maximum velocity of swimming is 0.06 m/s when the feathering frequency is 0.53 Hz. Maximum swimming number is 0.24 when the frequency is 0.35 Hz.
3. Vehicle velocity was estimated using the blade element theory. The result was 0.18 m/s when the flapping frequency is 0.53 Hz; this estimation is faster than the

experimental result. This is because of some assumptions for the estimation, and improvements of estimation should be done.

There are many flaws and issues in this vehicle. As it swims slower than expected, improvement of swimming performance by smoothing the motion of fore fins and an appropriate choice of angle of attack is required. It should also make use of the hind fins and the buoyancy controller. It does not dive into underwater with its own power yet, although the three-dimensional swimming is one of its main targets. By coping with these issues, the vehicle will provide better performance, and will be used to evaluate the usefulness of submergence vehicles with flapping fins.

## REFERENCES


[1] Triantafyllou, M. S., Triantafyllou, G. S. and Yue, D. K. P., Ann. Rev. Fluid Mech. Vol. 32, (2000), pp. 33-53.

[2] Hirata, K. et al., Proc. 1st Int. Symp. on Aqua Bio-Mechanisms, (2000), pp.287-292.

[3] Hirata, K., Proc. 6th Int. Symp. on Marine Eng., (2000), pp.711-714.

[4] Hishinuma, K. et al., Proc. 7th Int. Symp. Marine Eng. (2005), Paper 84, CD-ROM.

[5] Sheldahl, R. E., and Klimas, P. C., SANDIA REPORT SAND80-2114, Sandia National Laboratories, (1981).


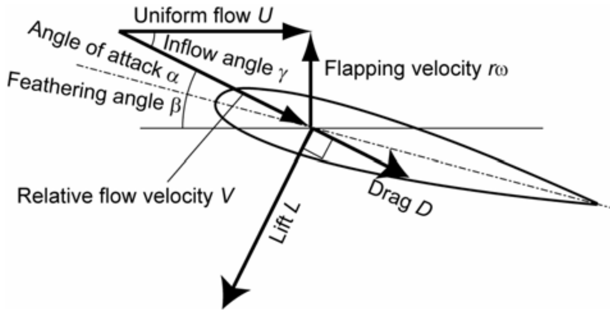


**Fig. 7: Definition of Variables**

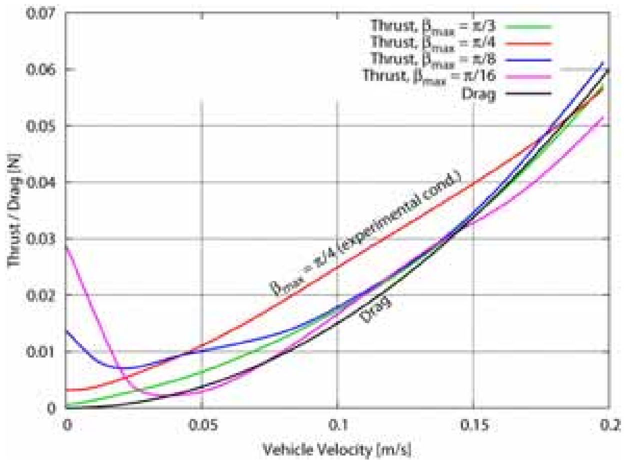


**Fig. 8: Thrust and Drag Forces as Functions of Vehicle Velocities. Flapping Frequency is 0.53 Hz.**